Research Article | Vol. 28, No. 16 / 3 August 2020 / Optics Express 23433
Optics EXPRESS

All-fiber spatiotemporally mode-locked laser with multimode fiber-based filtering

UĞUR TEĞIN,[1,2,*] BABAK RAHMANI,[2] EIRINI KAKKAVA,[1] DEMETRI PSALTIS,[1] AND CHRISTOPHE MOSER[2]

[1] Optics Laboratory, École Polytechnique Fédérale de Lausanne, Switzerland
[2] Laboratory of Applied Photonics Devices, École Polytechnique Fédérale de Lausanne, Switzerland
[*] ugur.tegin@epfl.ch

Abstract: We demonstrate the first all-fiber multimode spatiotemporally mode-locked laser. The oscillator generates dissipative soliton pulses at 1036 nm with 12 mW average power, 6.24 ps duration, and 24.3 MHz repetition rate. The reported pulse energy (0.5 nJ) represents ~4 times improvement over the previously reported single-mode all-normal dispersion mode-locked lasers with multimode interference-based filtering. Numerical simulations are performed to investigate the cavity and spatiotemporal mode-locking dynamics. The all-fiber oscillator we present shows promise for practical use since it can be fabricated simply.

1. Introduction

Ytterbium-based fiber laser systems are used in optical metrology, material processing and medical applications due to their high and broadband gain [1]. Unlike the other conventionally used gain elements (Er, Tm and Ho), the emission wavelength of an Ytterbium-doped silica fiber falls in a spectral range that exhibits positive group velocity dispersion ($\beta 2 > 0$), thus mode-locking is relatively challenging at 1 um wavelength. By using dispersion-management with gratings or photonic crystal fibers, soliton [2], dispersion-managed soliton [3] and similariton [4] pulse types were reported with Ytterbium-based single-mode fiber lasers. Later, all-normal dispersion mode-locking with spectral filtering of chirped pulses was discovered and depending on the filtering effect, either dissipative soliton [5] or amplifier similariton [6] pulses can be produced. Over the last decade, all-normal-dispersion fiber lasers have been studied mainly by employing dissipative soliton pulse dynamics [7]. These pulses are energy scalable and dissipative solitons with up to μJ pulse energies were demonstrated with custom made very-large mode area single-mode fibers [8].

All-fiber laser designs are a subject of high interest due to their compact and alignment-free operation. To achieve dissipative soliton pulses in an all-fiber configuration various inline fiber-based filtering solutions with >6 nm bandwidth have been reported in the literature [9–12]. Among them, multimode interference (MMI) based bandpass filtering is a convenient solution. Such a filter consists of a section of graded-index multimode fiber (GRIN MMF) between single or few-mode fibers. Interference effects between the modes introduces frequency-dependent sinusoidal transmission which can be used as a spectral filter [13]. Recently, dissipative soliton pulse formation with 0.13 nJ energy was presented in an all-fiber configuration with the multimode interference-based bandpass filtering in a single-mode Ytterbium-based all-normal dispersion laser [14].

In the last few years, spatiotemporal mode-locking is demonstrated by harnessing the unique properties of GRIN MMFs such as low modal dispersion and periodic self-imaging by Wright et al. and dissipative soliton pulses [15]. With the mode-locking approach in a multimode laser cavity, coherent superposition of transverse and longitudinal modes is demonstrated. By introducing spatial interactions to mode-locking mechanism complex multimode nonlinear wave propagation studies became feasible under partial feedback conditions. Later, observation of bound-state

#399668 https://doi.org/10.1364/OE.399668
Journal © 2020 Received 9 Jun 2020; revised 15 Jul 2020; accepted 16 Jul 2020; published 22 Jul 2020

Optics EXPRESS

solitons and harmonic mode-locking were reported with similar cavity orientations [16,17] and all-fiber cavity with SESAM mode-locking [18]. Recently, self-similar pulse propagation is reported in spatiotemporally mode-locked multi-mode fiber laser and observed output beam quality improvements with the temporal change [19]. By tailoring spatiotemporal nonlinear pulse propagation, intracavity Kerr-induced self-beam cleaning is achieved in a multimode laser cavity with sub-100 fs pulse duration, >20 nJ pulse energy and M2 value less than 1.13 [20].

The novelty in the current paper is the use of multimode fiber interference-based filtering to construct an all-fiber spatiotemporally mode-locked laser. With this alignment-free, compact cavity design, spatiotemporally mode-locked dissipative soliton pulse generation is demonstrated. Numerical simulations are performed to reveal cavity and spatiotemporal mode-locking dynamics and led to experimental studies. The experimentally demonstrated multimode laser is self-starting and generates pulses with 0.5 nJ energy, 12 mW average power, 6.24 ps duration and 24.3 MHz repetition rate at 1036 nm. With spatiotemporal mode-locking, the achieved pulse energy represents ~4 times improvement over the previously reported single-mode mode-locked all-normal dispersion lasers with multimode interference-based filtering.

2. Numerical results

The schematic of the all-fiber spatiotemporally mode-locked oscillator is presented in Fig. 1(a). The cavity consists of a step-index Ytterbium-based MMF segment with 10 µm core diameter, GRIN MMF segments with 50 µm core diameter and step-index passive MMF segments with 10 µm core diameter. The fiber sections with 10 µm core diameter support 3 modes and the GRIN MMF sections with 50 µm core diameter support ~240 modes at and around 1030 nm wavelength. Numerical simulations are performed to define lengths of the fiber segments, the bandwidth for multimode interference-based bandpass filtering and the possibility of spatiotemporal mode-locking in the presented cavity design.

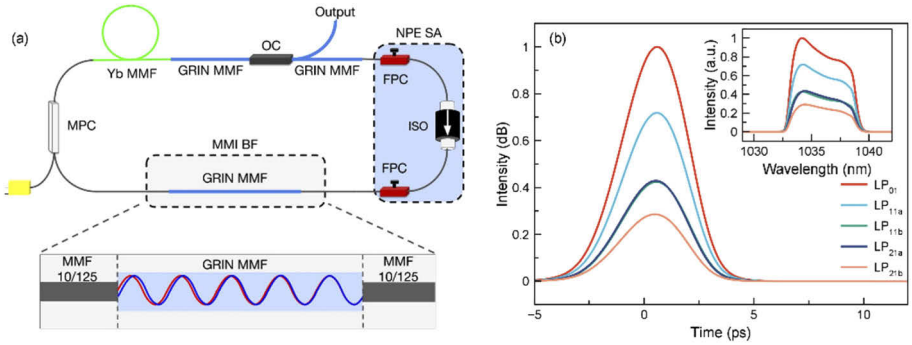

Fig. 1. (a) Schematic of the all-fiber spatiotemporally mode-locked laser with multimode fiber-based filtering: ISO, isolator; FPC, fiber polarization controller; OC, output coupler; MMI BF, multimode interference-based bandpass filter; MPC, multipump combiner. (b) Simulated mode-resolved temporal profile. Inset: Simulated mode-resolved spectral profile.

Simulations are conducted with the numerical model used by Teğin et al. [19,20]. The GRIN MMF segments are modeled with linearly polarized modes and the nonlinear multimode Schrödinger equation is simulated for these segments [21]. To decrease the computation time, GRIN MMF segments are considered with five modes (LP01, LP11a, LP11b, LP21a and LP21b), step-index MMF segments with few-modes are considered as single-mode. Only a small portion of the modes (5 out of 250) are included in the simulation due to computational limitations however we will show that this simplified model captures essential features of the behavior of the pulse propagation inside the laser. The step size of simulation was chosen as ~140 µm (quarter

Optics EXPRESS

of the self-imaging period, 560 µm) for the GRIN MMF and 0.5 cm for few-mode fiber segments with a time resolution of 80 fs with 24 ps time window width. The splice points were modeled by coupling coefficients of the modes before and after the GRIN MMF segments. The initial field in simulations is defined as a quantum noise and stable mode-locking regimes are found to be not critically dependent on the details of the coupling coefficients. The gain is modeled as Lorentzian shape with 30 dB small-signal gain and 40 nm gain bandwidth. The saturable absorber is modeled by a sinusoidal transfer function with 1 kW saturation power and 60% modulation depth.

The numerically achieved spatiotemporally mode-locked pulse shape and spectrum at the 30% output coupler are presented in Fig. 1(b). We set the excitation coefficients of the single mode section to the 5 mode GRIN MMF segments equal to [0.35, 0.25, 0.15, 0.15, 0.1] and the gain saturation energy as 1.10 nJ. It is known that in order to achieve dissipative soliton pulses in all-normal dispersion cavities bandpass filtering of chirped pulses with >6 nm bandwidth is required [5]. To ensure dissipative soliton mode-locking, we select the length of the GRIN MMF segment used for MMI filtering to be 25 cm which yields an 8 nm bandwidth bandpass filter [13]. In our simulations, dissipative soliton pulses with 0.46 nJ pulse energies and 5 nm spectral bandwidths were achieved. The output pulse duration was 3.6 ps at the output port. To understand the pulse propagation in detail, propagation of the pulse in one roundtrip is calculated and presented in Fig. 2. Due to the relatively high nonlinearity, the spectral broadening is observed in gain MMF segment which later reaches a steady-state value inside the GRIN MMF. As expected from dissipative soliton pulses in an all-normal dispersion cavity, the spectral broadening ratio in one roundtrip is small [22]. The output beam profile with the numerically

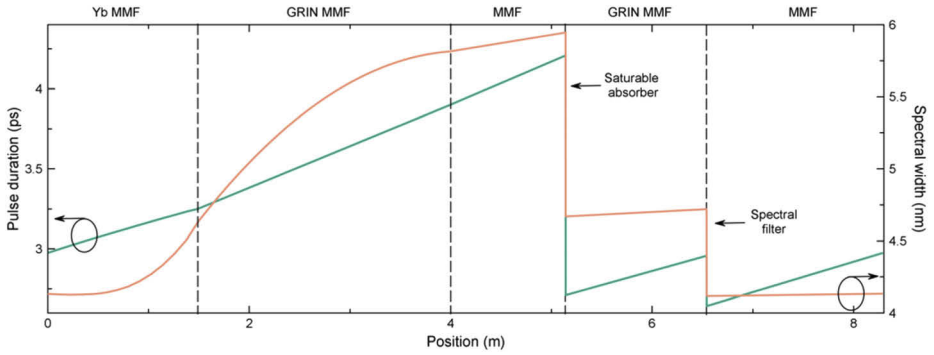

Fig. 2. Simulated pulse duration and spectral bandwidth variation over the cavity.

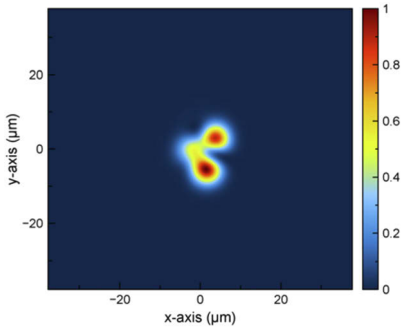

Fig. 3. Numerically obtained output beam profile.

Optics EXPRESS

calculated mode-locked field is presented in Fig. 3. Although most of the energy remains in the lower order modes, the numerically obtained output beam exhibits multimode features.

3. Experimental results and discussion

Encouraged by the simulations, experiments were performed with the numerically designed cavity parameters. The gain section of the oscillator is 1.5 m Yb MMF (nLight Yb-1200-10/125) pumped with a 976 nm pump diode coupled to the cavity with a pump combiner with matching passive fiber ports. The gain section is followed by a GRIN MMF based coupler with a 30% output coupling ratio. The modelocking mechanism is achieved by nonlinear polarization evolution (NPE) with a polarization-sensitive inline isolator with 10 um core diameter fiber and fiber polarization controllers. After the isolator and before the MPC, a 25 cm GRIN MMF with 50 µm core diameter is placed to achieve MMI bandpass filtering with 8 nm bandwidth. The experimental oscillator is shown in Fig. 4(a).

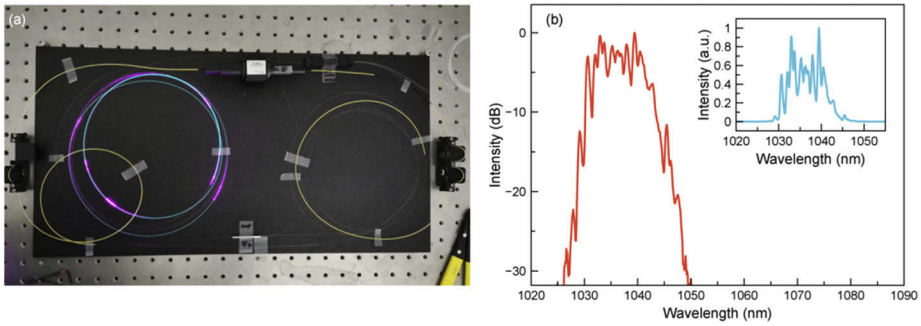

Fig. 4. (a) Experimental setup of the all-fiber spatiotemporally mode-locked laser with multimode fiber-based filtering. (b) Measured mode-locked spectrum in logarithmic scale. Inset: Measured mode-locked spectrum in linear scale.

Spatiotemporal mode-locking is achieved easily by adjusting the intracavity polarization with fiber the polarization controllers for 2.75 W pump power. The recorded spectra from the output coupler are presented in Fig. 4(b) with spectral 10 nm spectral width at 1036 nm central wavelength. The presented spectrum is measured with a 0.5 nm resolution and features a jagged profile. Similar behavior is reported for spatiotemporally mode-locked lasers and lasers with MMI segments. The reason for the jagged spectrum can be related to the aforementioned operation type and filtering. The self-starting mode-locking operation of a single-pulse train with 24.29 MHz is presented in Fig. 5(a). The output power of the laser is measured as 12 mW which corresponds to ~0.5 nJ pulse energy. The temporal characterizations are performed with second-order nonlinear autocorrelation. The laser produces chirped pulses with 6.24 ps pulse duration (see Fig. 5(b)).

It is important to consider the effect of the fiber length and diameter of the output coupler to laser output properties. The pulses propagate through 50 cm GRIN MMF with 50 um core diameter after leaving the oscillator. This output fiber causes highly multimode propagation with 0.5 nJ pulses and as presented in Fig. 6(a), the near field measurement of the output beam profile is speckled. In addition to its spatial effect, such a multimode propagation can cause temporal changes as well. Numerical simulations suggest an output pulse duration ~4 ps but experimental measurements indicated around 6 ps larger pulse duration. This 2 ps difference can be the result of the highly multimode propagation caused by the output coupler in addition to the differences caused by the simplified numerical model. The oscillator is also characterized in the frequency domain with a radio frequency for stability purposes. The fundamental repetition rate of the laser

Optics EXPRESS

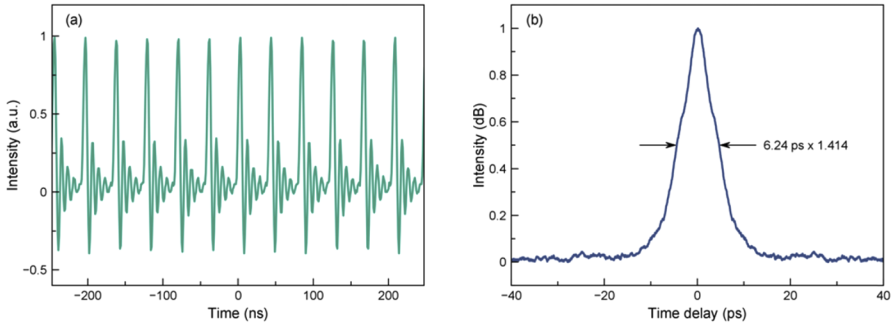

Fig. 5. (a) Measured single-pulse train of the spatiotemporally mode-locked laser. (b) Autocorrelation trace of the chirped pulse obtained from 50 cm GRIN MMF of output coupler.

is verified with a radio frequency (RF) analyzer (HP 3585A) as 24.29 MHz. With 1 kHz span and 10 Hz resolution bandwidth, a sideband suppression ratio around 70 dB is measured (Fig. 6(b)). The fiber laser has outstanding stability both in the short and long term. The laser continues the mode-locking operation uninterrupted for months, without a sign of degradation.

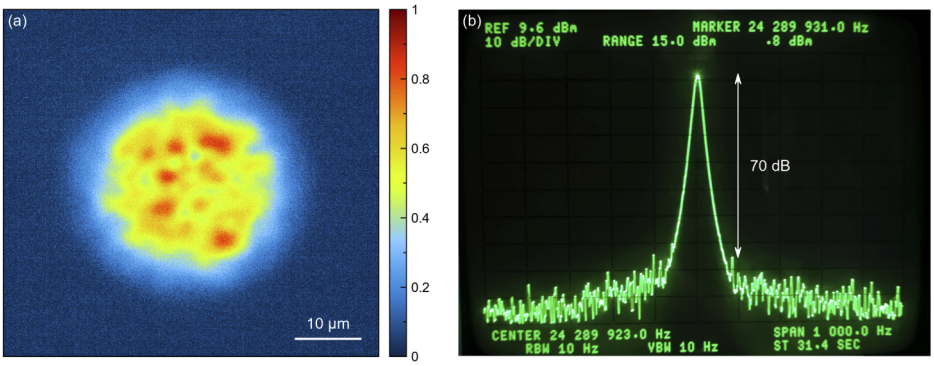

Fig. 6. (a) Measured near-field beam profile from 50 cm GRIN MMF of output coupler. (b) Measured radio frequency spectrum with 1 kHz span and 10 Hz resolution bandwidth.

4. Conclusion

In conclusion, we numerically and experimentally demonstrate an all-fiber spatiotemporally mode-locked laser with multimode fiber interference-based filtering. The Ytterbium-based all-normal dispersion multimode oscillator generates 6.24 ps pulses with 0.5 nJ pulse energy, 12 mW average power and 24.3 MHz repetition rate. Compared to Ytterbium-based single-mode mode-locked lasers with multimode interference-based filtering, the reported spatiotemporally mode-locked laser produces ~4 times more powerful pulses. The all-fiber cavity design provides high stability due to the inherent alignment-free construction. We believe the proposed cavity presents an alternative approach to achieve spatiotemporal mode-locking with a simple, all-fiber design that can be used when a clean Gaussian beam is not required such as speckle interferometry and structured illumination applications.

Disclosures

The authors declare no conflicts of interest.

Optics EXPRESS

References

1. M. E. Fermann and I. Hartl, "Ultrafast fibre lasers," Nat. Photonics **7**(11), 868–874 (2013).
2. A. Isomäki and O. G. Okhotnikov, "Femtosecond soliton mode-locked laser based on ytterbium-doped photonic bandgap fiber," Opt. Express **14**(20), 9238–9243 (2006).
3. B. Ortaç, A. Hideur, T. Chartier, M. Brunel, C. Özkul, and F. Sanchez, "90-fs stretched-pulse ytterbium-doped double-clad fiber laser," Opt. Lett. **28**(15), 1305–1307 (2003).
4. FÖ İlday, J. R. Buckley, W. G. Clark, and F. W. Wise, "Self-similar evolution of parabolic pulses in a laser," Phys. Rev. Lett. **92**(21), 213902 (2004).
5. A. Chong, J. Buckley, W. Renninger, and F. Wise, "All-normal-dispersion femtosecond fiber laser," Opt. Express **14**(21), 10095–10100 (2006).
6. W. H. Renninger, A. Chong, and F. W. Wise, "Self-similar pulse evolution in an all-normal-dispersion laser," Phys. Rev. A **82**(2), 021805 (2010).
7. P. Grelu and N. Akhmediev, "Dissipative solitons for mode-locked lasers," Nat. Photonics **6**(2), 84–92 (2012).
8. M. Baumgartl, C. Lecaplain, A. Hideur, J. Limpert, and A. Tünnermann, "66 W average power from a microjoule-class sub-100 fs fiber oscillator," Opt. Lett. **37**(10), 1640–1642 (2012).
9. M. Schultz, H. Karow, O. Prochnow, D. Wandt, U. Morgner, and D. Kracht, "All-fiber ytterbium femtosecond laser without dispersion compensation," Opt. Express **16**(24), 19562–19567 (2008).
10. K. Özgören and FÖ İlday, "All-fiber all-normal dispersion laser with a fiber-based Lyot filter," Opt. Lett. **35**(8), 1296–1298 (2010).
11. T. Walbaum and C. Fallnich, "Multimode interference filter for tuning of a mode-locked all-fiber erbium laser," Opt. Lett. **36**(13), 2459–2461 (2011).
12. L. Zhang, J. Hu, J. Wang, and Y. Feng, "Tunable all-fiber dissipative-soliton laser with a multimode interference filter," Opt. Lett. **37**(18), 3828–3830 (2012).
13. A. Mafi, P. Hofmann, C. J. Salvin, and A. Schülzgen, "Low-loss coupling between two single-mode optical fibers with different mode-field diameters using a graded-index multimode optical fiber," Opt. Lett. **36**(18), 3596–3598 (2011).
14. U. Teğin and B. Ortaç, "All-fiber all-normal-dispersion femtosecond laser with a nonlinear multimodal interference-based saturable absorber," Opt. Lett. **43**(7), 1611–1614 (2018).
15. L. G. Wright, D. N. Christodoulides, and F. W. Wise, "Spatiotemporal mode-locking in multimode fiber lasers," Science **358**(6359), 94–97 (2017).
16. H. Qin, X. Xiao, P. Wang, and C. Yang, "Observation of soliton molecules in a spatiotemporal mode-locked multimode fiber laser," Opt. Lett. **43**(9), 1982–1985 (2018).
17. Y. Ding, X. Xiao, P. Wang, and C. Yang, "Multiple-soliton in spatiotemporal mode-locked multimode fiber lasers," Opt. Express **27**(8), 11435–11446 (2019).
18. H. Wu, W. Lin, Y. Tan, H. Cui, Z. Luo, W. Xu, and A. Luo, "Pulses with switchable wavelengths and hysteresis in an all-fiber spatio-temporal mode-locked laser," Appl. Phys. Express **13**(2), 022008 (2020).
19. U. Teğin, E. Kakkava, B. Rahmani, D. Psaltis, and C. Moser, "Spatiotemporal self-similar fiber laser," Optica **6**(11), 1412–1415 (2019).
20. U. Teğin, B. Rahmani, E. Kakkava, D. Psaltis, and C. Moser, "Single mode output by controlling the spatiotemporal nonlinearities in mode-locked femtosecond multimode fiber lasers," arXiv preprint arXiv:2005.06761 (2020).
21. A. Mafi, "Pulse propagation in a short nonlinear graded-index multimode optical fiber," J. Lightwave Technol. **30**(17), 2803–2811 (2012).
22. W. H. Renninger, A. Chong, and F. W. Wise, "Dissipative solitons in normal-dispersion fiber lasers," Phys. Rev. A **77**(2), 023814 (2008).